Fission-like yields in $^{16}O + ^{40,44}Ca$ reactions

S. J. Sanders, R. R. Betts, I. Ahmad, K. T. Lesko,* S. Saini,† and B. D. Wilkins
Argonne National Laboratory, Argonne, Illinois 60439

F. Videbaek
Argonne National Laboratory, Argonne, Illinois 60439
and Niels Bohr Institute, University of Copenhagen, DK-2100 Copenhagen Ø, Denmark

B. K. Dichter‡
A. W. Wright Nuclear Structure Laboratory, Yale University, New Haven, Connecticut 06511
(Received 29 August 1985; revised manuscript received 21 July 1986)

Inclusive cross sections for the $^{16}O + ^{40}Ca$ reaction leading to fission-like fragments with mass $20 \leq A_{\text{fragment}} \leq 28$, and for the $^{16}O + ^{44}Ca$ reaction with $20 \leq A_{\text{fragment}} \leq 30$, have been determined by measurements at seven energies with $69.3 \leq E_{\text{lab}}(^{16}O) \leq 87.3$ MeV and for $30° \leq \theta_{\text{lab}} \leq 60°$. The evaporation-residue cross sections were also measured over a limited angular range at the same energies to search for any gross difference between these cross sections for the two systems. No difference was detected outside the experimental uncertainties. The resulting energy spectra and mass distributions for the fission-like yields are shown to be consistent with a fusion-fission reaction mechanism. Although it was not possible to determine the total fission-like cross sections since the apparent mass range of the fission-like yields was greater than that covered by the experiment, the magnitude and energy dependence of the observed fission-like cross sections, as compared to the evaporation-residue cross sections, are also found to be consistent with a fusion-fission mechanism.

I. INTRODUCTION

The fusion-fission process, in which the compound system formed by the fusion of two heavy ions subsequently fissions, has received considerable attention in studies of reactions involving systems with combined mass $A > 100$,[1-3] and some evidence for this process has been developed for systems as light as $A \simeq 80$.[4-8] In still lighter systems it has generally been assumed that the compound systems populated through fusion subsequently decay by the emission of light particles and γ rays. For these lighter systems the fusion cross sections are almost always equated with the measured evaporation residue (ER) cross sections. The observation of fission-like yield from reactions populating systems of total mass $A = 46$–64 (Refs. 9–11) indicates that a fusion-fission process may also play a role in these lighter systems. Recent measurements in this mass range[9-12] have been analyzed using quite different assumptions as to the origin of this yield—in general either a fusion-fission, or a deep-inelastic scattering origin is assumed. The basic difference in these pictures is that for the fusion-fission model it is assumed that an equilibrated compound nucleus is formed. Ritzka *et al.*,[12] in studying strongly damped yields from the $^{16}O + ^{48}Ti$ reaction, have analyzed their results in terms of a deep-inelastic scattering process. They find the angular distributions of this yield for the projectile-like fragments are forward peaked, with a slope that decreases with increasing angle. Decomposing the angular distributions into near-side, far-side, and orbiting contributions (using γ-ray circular polarization data), they attribute one-third of the total deep-inelastic cross section to an orbiting contribution with a $1/\sin\theta$ angular dependence. Alternatively, Grotowski *et al.*[10] in measuring symmetric products from the $^{12}C + ^{40}Ca$, $^{9}Be + ^{40}Ca$, and $^{6}Li + ^{40}Ca$ reactions have found that the measured fragment energies, as well as an excitation function for the $^{12}C + ^{40}Ca$ system, are consistent with a compound nucleus formation and decay process (fusion-fission). A recent study of the $^{58}Ni + ^{58}Ni$ reaction at 15.3 MeV/u incident energy by Awes *et al.*[13] also indicates a secondary, fission-like decay of the reaction fragments with $A \sim 56$.

The possible importance of a fission mechanism in the production of symmetric fragments has also been suggested in connection with the observation of narrow resonances in excitation functions for these fragments in the $^{28}Si + ^{28}Si$ and $^{24}Mg + ^{24}Mg$ systems.[14,15] The narrow resonances have many properties consistent with their identification as high-spin shape isomers which decay by fission, implying the importance of the fission process in these light nuclei.

One aspect regarding light nuclei which is less debatable than the possibility of a fusion-fission reaction mode is the importance of the spin value where the fission barrier vanishes. This sets an upper limit on the amount of spin a compound nucleus can have. The experimental signature for this limitation, a fall off of the fusion yield at high energies, has been observed in a number of studies.[16] For spin values near that where the barrier vanishes, it is reasonable to expect competition between fission and particle evaporation.

This paper reports on a measurement of the large-angle

reaction yields for the $^{16}O+^{40}Ca$ and $^{16}O+^{44}Ca$ systems conditioned on one of the reaction products having a mass intermediate between the target and projectile masses. These near-symmetric products for each system were measured at a number of laboratory energies in the range 69.3 MeV $\leq E_{lab} \leq$ 87.3 MeV. In a fusion-fission interpretation, the energy dependence of the fission cross sections, and the differences in these cross sections between the two systems, can be related to the different fission barriers of the systems. Concurrent measurements of the evaporation-residue yields for the two systems were also performed. By showing that the evaporation-residue cross sections are similar, any system dependence in the fission cross sections can be more directly related to differences in the predicted fission barriers. Although the fission-like yield was found to extend to mass-asymmetric channels, where it could not be clearly resolved from quasielastic scattering and processes resulting from target contaminants, with the consequence that only a qualitative comparison of theoretical expectations with experimental results is possible, the results of these measurements are found to be consistent with a fusion-fission picture.

The organization of this paper reflects the overall objective of developing evidence for the occurrence of the fusion-fission process in systems as light as $A=56$. After describing the details of the experimental procedure and the experimental results in Secs. II and III, respectively, in Sec. IV the data are discussed in the context of a fusion-fission model. The exit-channel total kinetic energies, mass distributions, and beam energy dependence of the fission-like yields are each shown to be consistent with the expectations of a fusion-fission picture. In this section the results of a calculation of the deep-inelastic scattering process are also presented. The limitations of the analysis and the present experimental data in firmly establishing the fusion-fission process in this mass range will be discussed. The paper concludes with a summary of the results, emphasizing the need for additional data.

II. EXPERIMENTAL PROCEDURE

The Argonne tandem-linac facility was used to produce a pulsed ^{16}O beam at energies $E_{lab}=69.3$, 73.8, 76.9, 80.6, 81.9, 82.8, and 87.3 MeV. The beam was incident on isotopically enriched targets of ^{40}Ca (180 μg/cm^2; 99.9% enrichment) and ^{44}Ca (150 μg/cm^2; $>85\%$ enrichment). The reaction products were detected in four 400 mm^2 Si (surface barrier) detectors located at $\theta_{lab}=30°$, 40°, 50°, and 60° and at a distance of 30 cm from the target. Each detector was collimated with a 2.11 cm diameter aperture for a solid angle of 3.9 msr corresponding to an angular acceptance of 4°.

Mass identification was accomplished by a time-of-flight measurement using the time structure of the beam. The time resolution for the ^{16}O beam pulses was $\sim$400 ps full width at half maximum (FWHM) with a spacing between pulses of 20.6 ns. The mass resolution for the observed fission-like fragments was approximately 2 mass units. Since unit mass resolution was not achieved, an initial mass calibration was accomplished using the centroids of the very intense ^{12}C and ^{16}O ridges in the energy versus time-of-flight spectra. Using this calibration it was possible to identify ridges near every fourth mass in the $^{16}O+^{40}Ca$ reaction. These ridges were assumed to correspond to the even-even, 4N nuclei ^{20}Ne, ^{24}Mg, ^{28}Si, etc.; the mass calibration was appropriately adjusted to obtain straight, horizontal ridges at every fourth mass in the calculated mass versus energy spectra. For the 30° detector it was possible to identify the mass lines up to the ^{40}Ca recoils. The mass calibration, which depends on the detector and the linac tuning parameters, does not, however, change for different targets at a given bombarding energy. The energy calibrations were determined by measuring the elastic-scattering yield from a thin Au target. The fragment energies were corrected for energy loss in the target, and in the detector dead layer (40 μg/cm^2 Au), and for the calculated pulse-height defect.[17] The uncertainties in the derived particle energies increase with increasing mass and for lower energy fragments. Using the Au energy calibration, the centroids of the $^{16}O + ^{40,44}Ca$ elastic-scattering peaks were found to be within 100 keV of the calculated energies. For extracting centroids of energy spectra near mass 28, the energy calibration is believed to be accurate to better than 1 MeV.

In order to monitor the evaporation-residue yields a ΔE-E telescope was positioned at angles slightly larger than the peak in the $d\sigma/d\theta$ (ER) distribution. This telescope subtended a solid angle of 0.06 msr and consisted of a 3.6 μm Si (surface barrier) ΔE detector and a 300 μm Si (surface barrier) E detector. For both targets, and at all but the lowest energy, ER measurements were taken at $\theta_{lab}=9°$, 11°, and 13°. At $E_{lab}=81.9$ MeV these measurements were extended back to $\theta_{lab}=21°$. The yields in the fission detectors and the ER telescope were normalized to the elastic-scattering yield in a monitor detector located at $\theta_{lab}=20°$.

III. EXPERIMENTAL RESULTS

A. Evaporation residue yields

The evaporation-residue yields were measured to check if any differences observed in the fission-like yields for the $^{16}O+^{40}Ca$ and $^{16}O+^{44}Ca$ systems could be related to differences in the overall fusion cross sections for the two systems. The $^{16}O+^{40}Ca$ ER cross sections have been measured previously over an extended energy range (including the energies of interest here) by Vigdor *et al.*[18] Since the present analysis would only be affected by major differences in the respective ER cross sections, no attempt was made to measure this yield to the small angles necessary to obtain total cross sections. Instead the ER cross sections were sampled for both targets at a consistent set of angles.

The ER angular distribution for the $^{16}O+^{40}Ca$ and $^{16}O+^{44}Ca$ reactions at $E_{lab}=81.9$ MeV are shown in Fig. 1(a). The cross sections for the two systems are found to be quite similar. Figure 1(b) shows excitation functions for the angle-integrated, ER cross sections ($9° \leq \theta_{lab} \leq 13°$). Again there is no evidence for any substantial differences developing between the two systems. The relatively constant cross sections as a function of energy reflect the fact

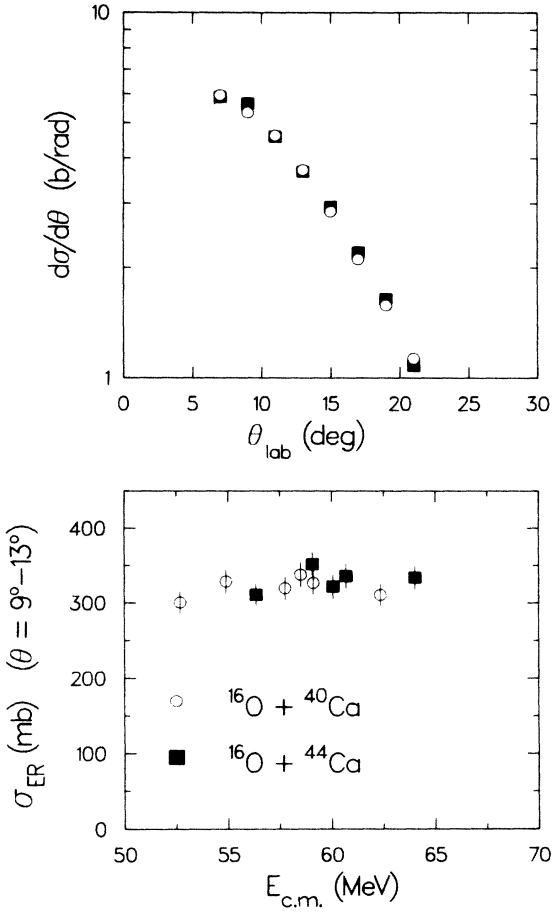

FIG. 1. Evaporation residue cross sections. The open circles are for the $^{16}O+^{40}Ca$ reaction and the filled squares are for the $^{16}O+^{44}Ca$ reaction. If not shown, the uncertainties are covered by the symbols. (a) Differential cross sections at $E_{lab}(^{16}O)=81.9$ MeV. (b) Excitation functions of angle integrated cross section ($9° \leq \theta_{lab} \leq 13°$).

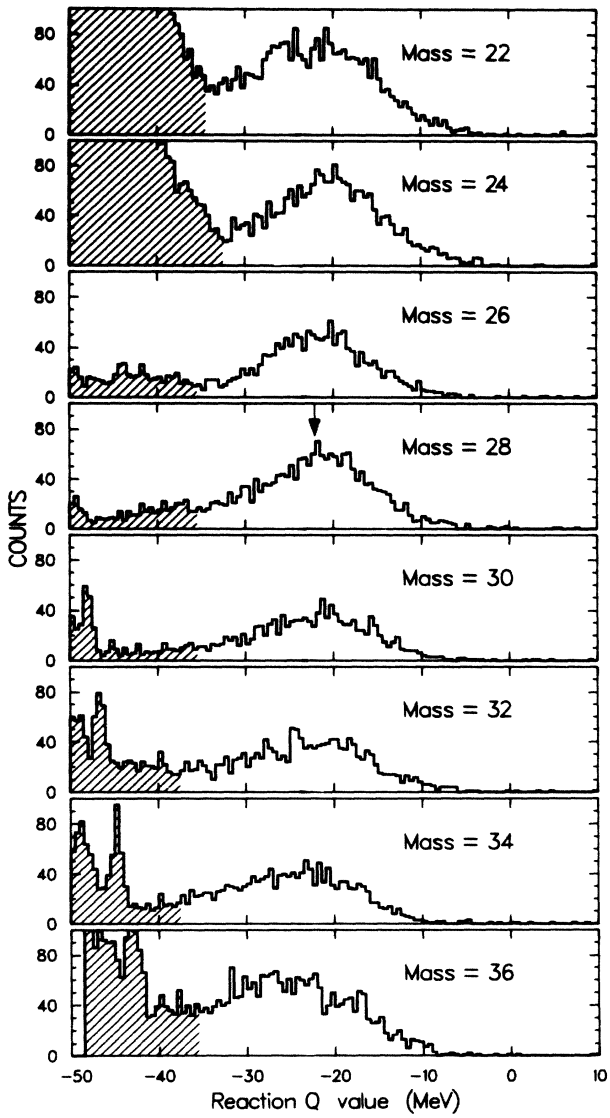

FIG. 2. Q-value spectra for the $^{16}O+^{40}Ca$ reaction leading to different mass fragments at $E_{lab}(^{16}O)=82.8$ MeV and $\theta_{lab}=30°$. The cross-hatch shading indicates regions of the spectra which are obscured by contaminant processes (see text). The arrow indicates the most probable Q value for the symmetric-fragment channel.

that the present measurements are at energies above that at which the ER cross sections have been found to saturate.[18]

B. Fission-like yields—energy spectra

From the two-dimensional spectra of mass versus energy, individual energy spectra for different mass ranges were obtained, with each new spectrum corresponding to a range of two mass units and centered on one of the even masses between 22 and 36 u. The binning of these spectra by two mass units reflects the experimental mass resolution. In Fig. 2 the energy spectra are shown for the different mass cuts in the $^{16}O+^{40}Ca$ reaction data at $E_{lab}(^{16}O)=82.8$ MeV and 30°. The Q-value scale was obtained assuming two-body kinematics using the mean mass values. There is a clear peak in each of the spectra near $Q=-22$ MeV corresponding to the fission-like yield. The increasing yields at very low Q values (indicated by the cross-hatch shading in the figure) can be attributed to two different causes. For the low-mass spectra ($A \leq 26$), this yield results from particle-evaporation channels in ^{16}O induced fusion on ^{12}C and ^{16}O target contaminants. For the heavier masses ($A \geq 28$) this yield is primarily a consequence of the spacing between beam pulses: in timing with respect to the linac beam structure, when the fragment flight time becomes longer than the spacing between beam pulses, there is a wrap-around observed in the time-of-flight versus energy spectrum. This can result in an experimental ambiguity between the identification of a slower, heavy fragment and a faster, light fragment of the same energy. Estimates were made of the fission-like yield obscured by these experimental causes (generally less than 30% of the total yield) in deriving cross sections. Figure 3 shows the resulting laboratory differential cross sections at 82.8 MeV. Relative uncer-

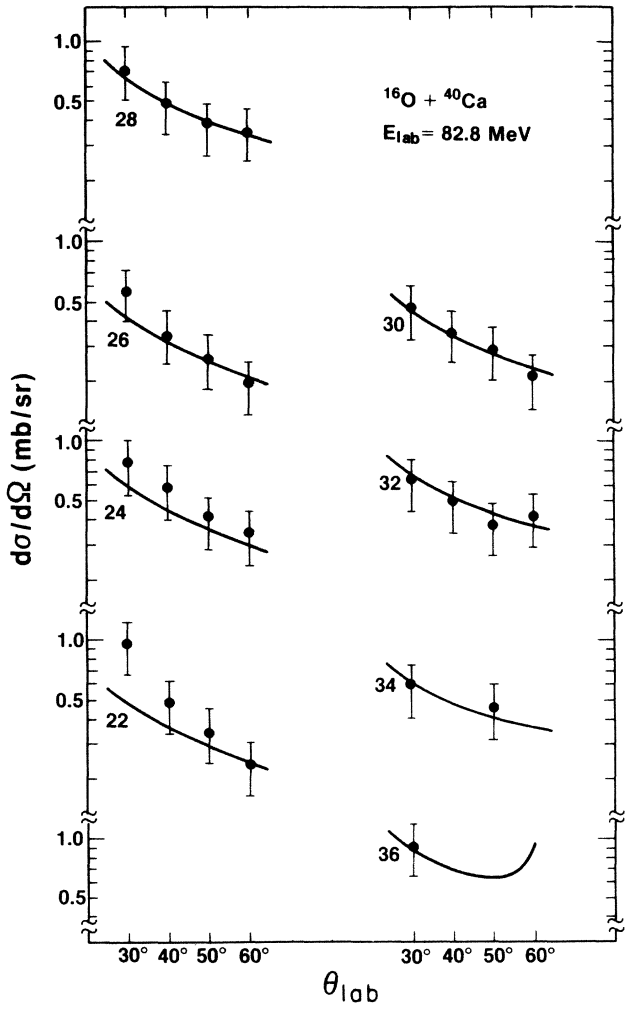

FIG. 3. Laboratory differential cross sections for the $^{16}O+^{40}Ca$ fission-like yield at 82.8 MeV. The numbers indicate the central mass value of the two-unit mass bins used in sorting the data. The curves, as discussed in the text, correspond to constant values of $d\sigma/d\theta$ (c.m.).

tainties of ±25% have been assigned to the cross sections reflecting the uncertainties involved in estimating the amount of yield missed at low fragment energies.

Two additional uncertainties arise in measuring the inclusive reaction yield in a singles experiment. It is unknown to what extent the observed yield results from two-body reactions, and it is also unclear how the observed mass distributions differ from the primary mass distribution as a result of light-particle evaporation from the primary fragments. Direct evidence does exist for the $^{16}O+^{40}Ca \rightarrow ^{28}Si+^{28}Si$ reaction at $E_{lab}=77$ MeV (Ref. 19) that, at least to a Q value of -20 MeV, the singles measurement does correspond to a primary mass distribution from a two-body reaction. This conclusion results from a comparison of singles and coincidence data obtained at this energy. (For more negative Q values the coincidence measurement had a sharp detection efficiency cutoff.) In their coincidence measurements of the $^{12}C+^{40}Ca$ reaction at 186 and 121 MeV, Grotowski *et al.*[10] found that the reaction to channels with a near-symmetric mass partition was two-body with an average loss of charge from secondary particle evaporation decreasing with energy from six to four charge units. It should be noted, however, that their measurements were carried out at considerably higher energies than the present one. Although secondary particle emission is possible from very low Q-value events, thus affecting the Q-value spectra and derived mass distributions, this process is unlikely to substantially change those features of the data on which the conclusions of the present work are based (i.e., the most-probable Q values, the qualitative mass distribution, and the total observed fission-like yield).

C. Fission-like yields—angular dependence

With the assumption that the primary fragments from a two-body reaction are being observed, it becomes possible to obtain both center-of-mass angular distributions and estimates of the total fission-like yield for different mass cuts. Reaction kinematics averaged over the Q-value distributions were used for the transformations from the laboratory to the center-of-mass (cm) systems. The angular distributions are found to follow largely a $1/\sin(\theta_{c.m.})$ angular dependence, with the exception of the lightest fragments at the most forward angles. This is shown for the $^{16}O+^{40}Ca$ reaction at $E_{lab}=82.8$ MeV in Fig. 4 where $d\sigma/d\theta_{c.m.}$ is plotted versus angle for the mass bins centered at 22, 24, 26, and 28 u (open circles); the filled squares represent cross sections derived from measurements of the corresponding heavy-reaction partners.

The horizontal lines in Fig. 4 indicate the angle-independent values of $d\sigma/d\theta_{c.m.}$ which were used to obtain the total cross sections for the fission-like yield. Similar distributions were obtained at the other energies and for the ^{44}Ca target. A constant value of $d\sigma/d\theta_{c.m.}$ [corresponding to a $1/\sin(\theta_{c.m.})$ distribution in $d\sigma/d\Omega$] is expected for the decay of any long-lived system where the relative angular momentum vector for the two fragments is both large and perpendicular to the reaction plane. These conditions are expected to be met for the fission of the systems studied here (see, for example, Ref. 20). In those cases where there was a forward rise observed in the $d\sigma/d\theta_{c.m.}$ distributions (as seen for the mass 22 and 24 cuts in Fig. 4), the larger-angle data were emphasized in determining the angle-integrated, fission-like cross sections. For these lighter masses there may well be contributions from quasielastic and possibly deep-inelastic processes which can result in additional cross section at forward angles. The curves in Fig. 3 result from converting back to the laboratory system the lines of constant $d\sigma/d\theta_{c.m.}$ displayed in Fig. 4. The integrated cross sections for the different mass bins are shown in Fig. 5 for both the ^{40}Ca and ^{44}Ca targets and for the different bombarding energies. It should be noted that the integrated cross section shown for the mass 20 bin is in all cases derived from a single 30° data point; this corresponds to the mass 36 yield in the $^{16}O+^{40}Ca$ reaction, and the mass 40

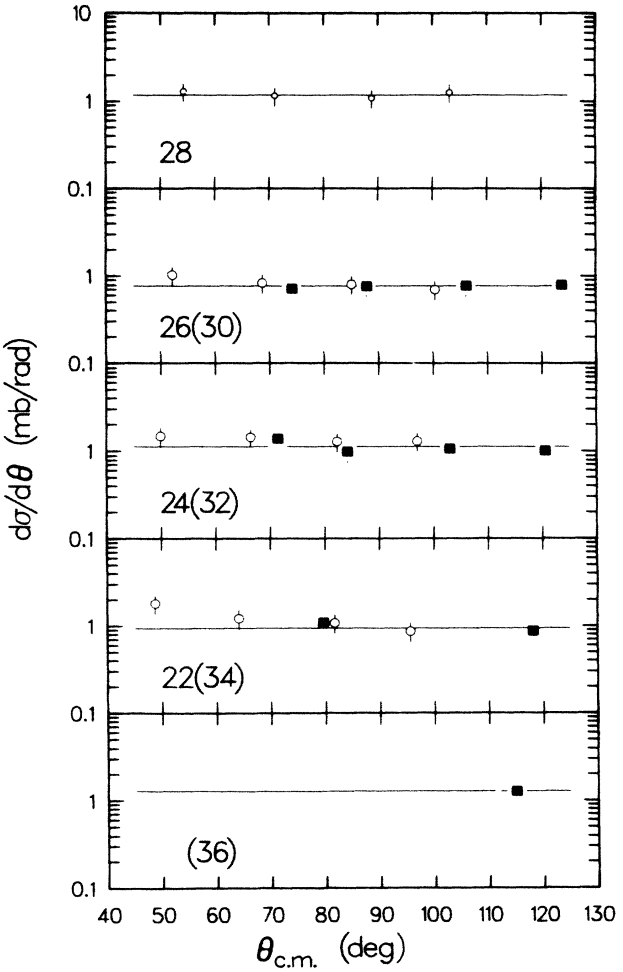

FIG. 4. Center-of-mass values of $d\sigma/d\theta$ for the $^{16}O+^{40}Ca$ reaction at $E_{lab}(^{16}O)=82.8$ MeV. Mass bins summing to the same compound nucleus mass 56 value are plotted together, with the heavier fragment plotted at the angle where its lighter partner would be expected assuming two-body kinematics. The open circles (closed squares) indicate the lighter (heavier) fragment. The mass 20 fission-like yield could not be cleanly resolved in the present experiment.

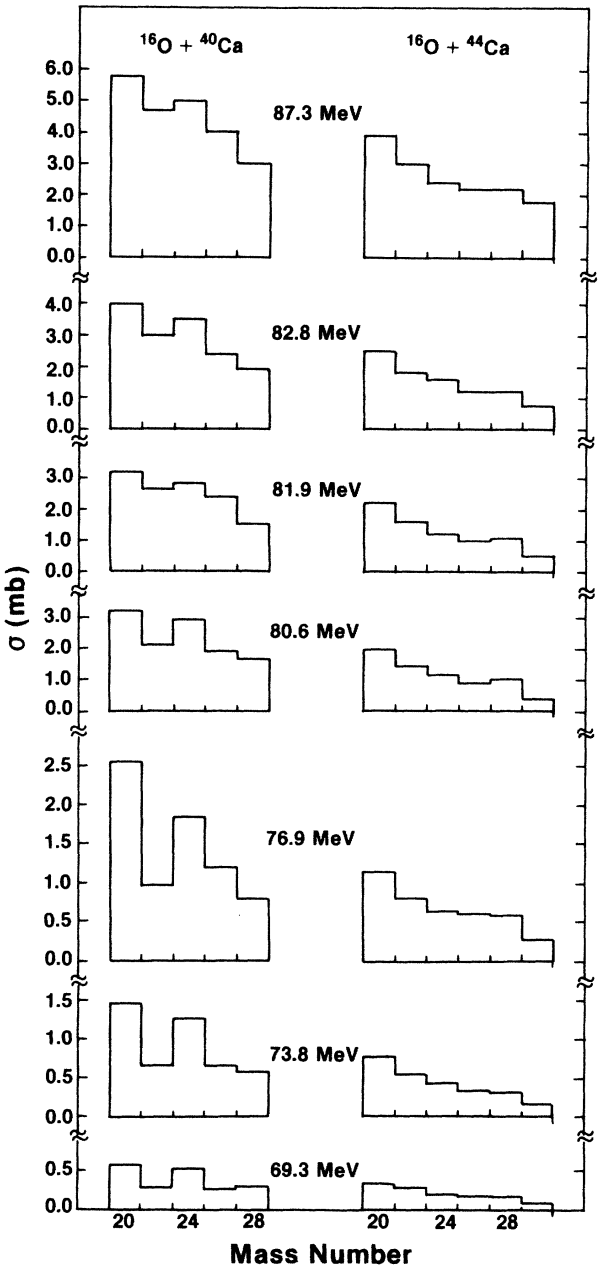

FIG. 5. Angle-integrated cross sections for the fission-like yield in the $^{16}O+^{40}Ca$ and $^{16}O+^{44}Ca$ reactions.

yield in the $^{16}O+^{44}Ca$ reaction. The mass 28 and mass 30 differential cross sections for the $^{16}O+^{40}Ca$ and $^{16}O+^{44}Ca$ reactions, respectively, have been halved in obtaining angle-integrated cross sections because of the double counting inherent to the experimental detection of symmetric fragments. The relative uncertainties in the integrated cross sections are determined largely by the uncertainties in the differential cross sections and are estimated to be ±25%.

The summed cross sections for the fission-like yields for the two systems are shown in Fig. 6 as functions of the respective center-of-mass energies. For the $^{16}O+^{40}Ca$ reaction the sum is for mass bins 20 to 28, and for the $^{16}O+^{44}Ca$ reaction the sum covers mass bins 20 to 30. The overall uncertainty is taken as 30% for each summed cross section.

IV. DISCUSSION

A. Reaction dynamics—characterization of data

The angular distribution data, as discussed previously, indicate the formation of a relatively long-lived, dinuclear complex. This may correspond to the formation of a compound nucleus followed by fission, or it could be related to an orbiting process in deep-inelastic scattering,[21] where one or more revolutions are completed before separation. In either case if it is assumed that the relative

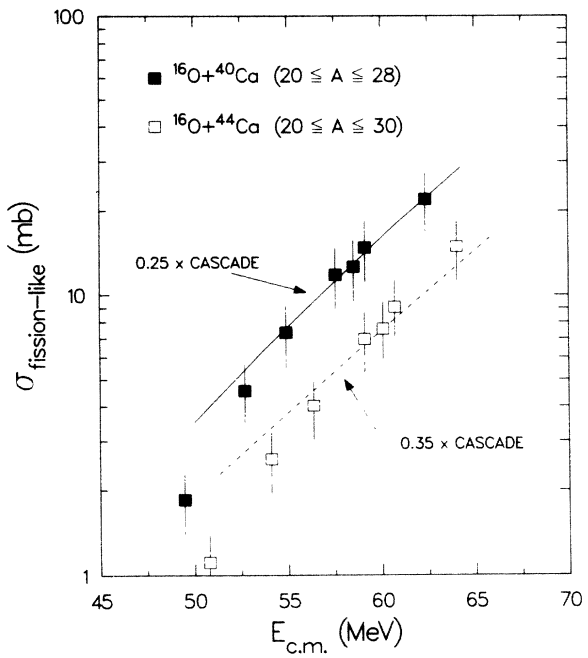

FIG. 6. Total observed fission-like cross sections for the $^{16}O+^{40}Ca$ and $^{16}O+^{44}Ca$ reactions. The range of fragment masses included in the yield is indicated. The lines indicate the calculated fission cross sections in these two systems as described in the text. The calculated cross sections have been scaled by the indicated amounts.

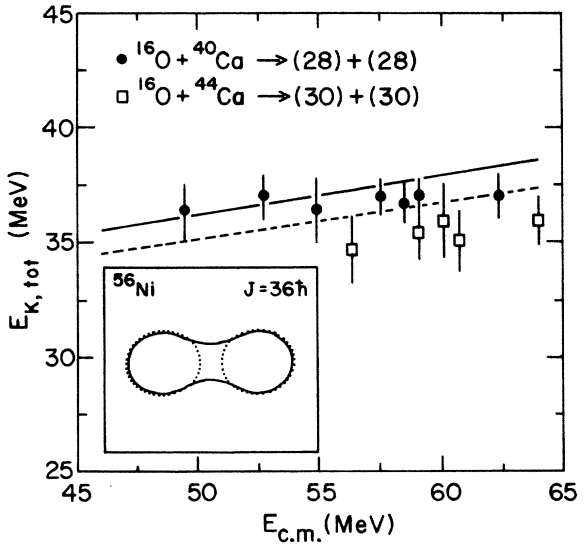

FIG. 7. Total kinetic energies ($E_{K,tot}$) observed in the symmetric-mass breakup channel for the $^{16}O+^{40}Ca$ reaction (solid circles) and the $^{16}O+^{44}Ca$ reaction (open squares). The solid line indicates the predicted values of $E_{K,tot}$ for the $^{16}O+^{40}Ca$ system, based on the liquid drop saddle point configuration and a fission angular momentum given by the critical angular momentum for fusion (see text). The dashed curve indicates the corrresponding values of $E_{K,tot}$ for the $^{16}O+^{44}Ca$ system. The sketch indicates the geometry of the two-spheroid approximation (dashed curves) and the corresponding rotating liquid drop model saddle-point shape (solid curve).

radial velocity of the two fragments vanishes at the point of separation, and furthermore that only conservative forces act between the fragments after separation, then the final total kinetic energy $E_{K,tot}$ of the fragments can be related to the potential and rotational energy at the point of separation.[22,23] The reaction Q value is simply the difference between the exit channel total kinetic energy and the incident center-of-mass energy, and consequently the Q-value spectra, which were generated for the different mass cuts, reflect the dynamics of the system at the point where the fragments separate.

In the present measurement the Q-value spectra all show a similar behavior with an approximately Gaussian shape from the most positive Q value to the peak of the distribution, and then a tail at low Q which falls off more slowly than expected for a Gaussian distribution. The present data are analyzed in terms of the most-probable Q values for the different spectra as defined by the peak of the Q distribution. The arrow in Fig. 2 indicates the most-probable Q value assigned to the mass 28 spectrum of the $^{16}O+^{40}Ca$ reaction at 82.8 MeV (based on measurements at all four angles). The most-probable Q values were used in this analysis rather than the mean Q values because of the uncertainties in extracting the latter as a result of energy thresholds. The most-probable Q values are also expected to be less sensitive to the effects of light-particle evaporation. The $E_{K,tot}$ values derived from the most-probable Q values obtained for the symmetric-fragment channels, $^{16}O+^{40}Ca \rightarrow ^{28}X+^{28}Y$ and $^{16}O+^{44}Ca \rightarrow ^{30}X+^{30}Y$, are shown in Fig. 7.

B. Reaction dynamics—fusion-fission

Assuming a fusion-fission mechanism, an estimate was obtained of the total kinetic energy in each symmetric-fragment channel by approximating the corresponding liquid drop model saddle-point configuration with two deformed spheroids and then determining the relative rotational and interaction energies (Coulomb + nuclear) of the spheroids. For light systems the difference in energy between saddle- and scission-point configurations is thought to be small[24] (low dissipation limit), so the asymptotically observed total kinetic energy should be comparable to the relative energy at the saddle point. The calculations of the saddle-point energies and shapes followed closely the procedures discussed in Refs. 25–28, explicitly including effects of the finite range of the nuclear force (using a Yukawa-plus-exponential nuclear energy) and diffuse surface corrections. The parameterization of the saddle-point shapes was in terms of three smoothly joined portions of quadratic surfaces of revolution, with two spheroids joined by a neck.[25] The equivalent spheroid geometry was obtained by absorbing the neck into the two end spheroids, retaining the deformation and centers separation of the end spheroids.

The rotational energies of the fissioning system were derived using the critical angular momenta for fusion, l_c, in the sharp-cutoff approximation. As will be discussed, in these light systems only the highest partial waves con-

tributing to fusion are expected to contribute to the fission yield. The parameter l_c was derived using a parametrization of the fusion cross section in terms of a critical radius parameter r_c and corresponding critical potential V_c, with r_c and V_c taken appropriate for the $^{16}O+^{40}Ca$ reaction from the work of Vigdor *et al.*;[18] this work also contains a discussion of the sharp-cutoff approximation. The same parameters were used in the calculation of l_c for the $^{16}O+^{44}Ca$ reaction. At a given c.m. energy this parameterization results in a calculated fusion cross section for the $^{16}O+^{44}Ca$ reaction which is 4% larger than the $^{16}O+^{40}Ca$ cross section—a difference to which the present measurement of evaporation-residue cross section would have been insensitive.

As an example of the relative energy values at the saddle point, for the $^{16}O+^{40}Ca\rightarrow^{28}Si+^{28}Si$ reaction at $E_{c.m.}=60$ MeV ($l\sim34\hbar$) the calculated relative energies are $V_{Coul}=27.8$ MeV, $V_{nucl}=-0.8$ MeV, and $E_{rot}(rel)=10.0$ MeV. The small value of V_{nucl} is consistent with the assumption that the scission and saddle point energies are quite similar in these systems. The solid curve in Fig. 7 shows the results of the $E_{K,tot}$ calculations for the $^{16}O+^{40}Ca\rightarrow^{28}Si+^{28}Si$ reaction; the dashed curve corresponds to the $^{16}O+^{44}Ca\rightarrow^{30}Si+^{30}Si$ reaction. These calculations are found to reproduce the magnitude and general energy dependence of $E_{K,tot}$ for the two systems reasonably well. Also shown in the figure are superimposed sketches of a typical saddle-point shape and the corresponding equivalent-spheroids geometry.

C. Mass distributions

The mass distributions, as shown in Fig. 5, indicate a tendency for both the $^{16}O+^{40}Ca$ and $^{16}O+^{44}Ca$ systems to break up into mass-asymmetric fragments. Apart from this similarity, there are notable differences in the fission-like yield for the two systems. As indicated previously, the cross sections for the ^{40}Ca target are generally higher. Also, the $^{16}O+^{40}Ca$ reaction shows a clear enhancement in the mass 20 and mass 24 channel cross sections which is not evident with the ^{44}Ca target.

It is not obvious what to expect for these mass distributions in terms of a fusion-fission process. The fissility of the ^{56}Ni and ^{60}Ni compound systems are well below the Businaro-Gallone point[29–31] marking the transition from symmetric to asymmetric fission for a spinless liquid drop. However, the high spin values of the ^{56}Ni and ^{60}Ni systems, as populated with the heavy-ion reactions $^{16}O+^{40}Ca$ and $^{16}O+^{44}Ca$, respectively, have the effect of lowering the mass value of this transition point. Saroha *et al.*[32] have calculated the mass distribution for the $^{16}O+^{40}Ca$ reaction at an incident energy of 75 MeV within the framework of a dynamical fragmentation theory. In this picture the stationary Schrödinger equation is written in terms of a collective mass asymmetry coordinate. Although experimental, ground-state binding energies were used in the calculation, and consequently the dynamics are different from what would be expected for nuclear fission, the calculation does suggest a relatively broad mass distribution as well as the importance of the 4N channels in the fragmentation of ^{56}Ni. Here a somewhat similar approach was taken to determine whether the presently observed mass distributions, and differences in these distributions for the $^{16}O+^{40}Ca$ and $^{16}O+^{44}Ca$ systems, are consistent with a fusion-fission picture. Calculations of the probability for different mass partitions were based on the phase space available in the partitions at the scission point.[33]

Several simplifying assumptions were made in the application of this scission-point model, and as such the resulting calculations must be viewed as being largely schematic. The probability for a given mass split was taken to be proportional to the product of the level densities in the two fragments as determined in the spheroid picture discussed in Sec. IV B. The energy available for internal excitation of the fragments was taken as the compound nucleus energy above the saddle point energy. To estimate the saddle-point energies for mass-asymmetric partitions, the double spheroid picture was first used to determine the difference in the relative energy of mass-asymmetric spheroids from the symmetric system value. This energy difference was then also taken as the change in the saddle-point energy going to the asymmetric system. The geometry of the mass-asymmetric spheroids was determined by first assuming a common spheroid deformation as calculated for the symmetric system. The separation of the spheroids was then found by requiring a balance of the relative nuclear, Coulomb, and centrifugal forces. The angular momentum of the fissioning system was taken as the critical angular momentum for fusion in a sharp-cutoff approximation. The calculated total excitation energy was then distributed between the fragments with mean values according to the inverse of the masses (constant temperature approximation), but with a Gaussian spread in the energy of each fragment. The variance of the Gaussian spreading distribution was taken as 3 MeV, although the resulting mass distributions were found to be quite insensitive to this value. Although the final fragment energies were not explicitly corrected for shell or pairing effects, these energies were adjusted by the Wigner term suggested by Myers and Swiatecki.[34] Fermi gas level densities were used with the moment-of-inertia of each fragment taken as the deformed spheroid value, and with a level density parameter (a) related to the fragment mass $A_{fragment}$ by $a=A_{fragment}/8$ (MeV^{-1}).

In Fig. 8 the calculated mass distributions for fusion-fission of the $^{16}O+^{40}Ca$ and $^{16}O+^{44}Ca$ systems at $E_{c.m.}=60$ MeV are shown. The mass bins are labeled by the lighter of the two fragments. Even with these very schematic calculations, several features are evident which can be compared to the experimental mass distributions (see Fig. 5). The calculated distributions are relatively flat near symmetry and favor an asymmetric mass distribution. The data clearly indicate an asymmetric distribution. In addition, the experimental enhancement of the 4N channels in the $^{16}O+^{40}Ca$ reaction is clearly evident in the calculations. This feature of the calculation is found to be a consequence largely of including the Wigner term in determining the final excitation energies. The Wigner term results in relatively greater binding for $N=Z$, even-even nuclei than in $N\neq Z$ nuclei and $N=Z$, odd-odd nuclei. In the fission of ^{56}Ni both fragments can be in a

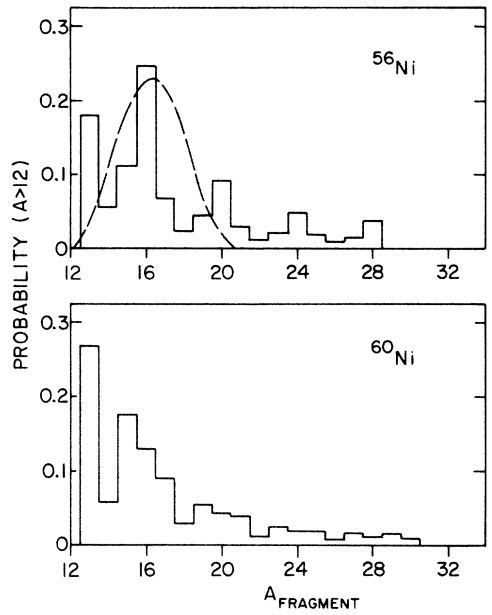

FIG. 8. Calculated mass distributions for ^{56}Ni and ^{60}Ni fission. Shown are the probabilities for different mass partitions using the schematic calculation discussed in the text. The dashed curve indicates the calculated deep-inelastic scattering mass distribution with $E_{c.m.} = 60.7$ MeV and $l = 36\hbar$.

"favored" configuration, whereas for ^{60}Ni fission only one of the fragments can be an $N = Z$, even-even nucleus.

These results suggest that the observed mass distributions are consistent with a fusion-fission process. They also suggest, however, that caution is needed in comparing the total observed fission-like yield for the two systems. It is clearly possible that the fraction of the total fission yield which is observed in the present experiment may be quite different for the two systems. The calculations are, unfortunately, much too schematic to be taken as reliable indicators of the amount of missed fission yield. Shell and pairing corrections to the binding energies of the fragments will certainly affect the calculated mass distribution, and the simplifying assumptions used for determining the asymmetric saddle energies are likely to be quite poor for the more asymmetric mass channels.

D. Cross sections

Fission cross sections for the $^{16}O + ^{40}Ca$ and $^{16}O + ^{44}Ca$ reactions can be calculated assuming that fission competes with light-particle evaporation in the decay of the respective ^{56}Ni and ^{60}Ni compound nuclei. The amount of fission relative to particle evaporation is determined by comparing the density of states at the saddle configuration to the sum of the level densities in the evaporation residues reached from the compound system, with the latter suitably scaled by the transmission coefficients for the different particle-evaporation channels. A modified version of the computer code CASCADE (Ref. 35) was used in calculating the fission yields for the two systems. The modification consisted of incorporating a subroutine by Sierk[27] which gives spin-dependent fission barriers corrected for the finite range of the nuclear force and surface-diffuseness effects.[29] These corrections result in substantially lower fission barriers for lighter systems,[29,30] and thus enhance the fission yield over estimates based on the standard rotating liquid drop model.

In these light systems the fission barriers are high at low spins. The $J = 0$ barriers for ^{56}Ni and ^{60}Ni are 45.9 and 48.6 MeV, respectively. As a consequence, low-spin states of the compound nucleus predominantly decay by light-particle evaporation and γ emission. It is only for the highest partial waves leading to fusion that the J-dependent fission barriers become low enough for fission to compete successfully with particle evaporation. The calculated fission yields are therefore very sensitive to the high-l tail of the fusion l distribution. In the present calculations the fusion partial cross sections were taken as

$$\sigma_l \propto (2l+1)/\{1+\exp[(l-l_0)/\Delta]\}$$

with $\Delta = 2\hbar$, and l_0 adjusted to give the same evaporation residue yield as calculated using the parametrization of Vigdor *et al.*[18] The fusion partial wave distribution is shown in Fig. 9 for the $^{16}O + ^{40}Ca$ reaction at $E_{c.m.} = 60.7$ MeV; also shown is the corresponding distribution of fission partial cross sections. It should be noted that l_0 differs from the previously discussed critical angular momentum l_c in that for l_0 the fission and evaporation-residue yields are summed to give the total fusion cross section. In general the difference in the two angular momenta increases with energy (and fission cross section), reaching a value of $l_0 - l_c = 1.3\hbar$ for the $^{16}O + ^{40}Ca$ system at the highest energy reached in the present experiment.

The calculated fission cross sections are shown on Fig. 6 for the $^{16}O + ^{40}Ca$ (solid line) and $^{16}O + ^{44}Ca$ (dashed line) reactions. The calculations have been scaled by factors of 0.25 and 0.35 for the two systems, respectively, to better enable a comparison of the experimental fission-like cross sections and the calculated fusion-fission cross sec-

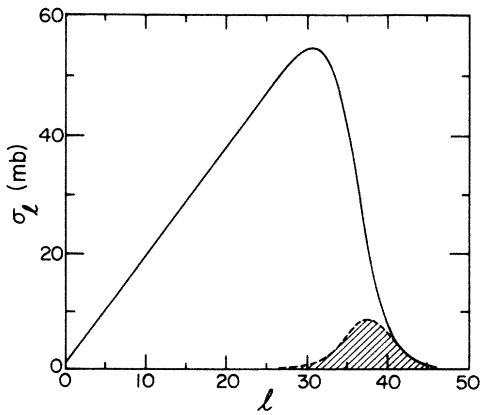

FIG. 9. Partial cross section distribution for fusion of the $^{16}O + ^{40}Ca$ system at $E_{c.m.} = 60.7$ MeV is indicated by the solid curve (as used in the CASCADE calculations discussed in the text). The shaded region indicates the corresponding fission partial cross sections.

tions. Changing the diffuseness of the assumed fusion l distribution (Δ) has a large effect on the magnitude of the calculated fission cross sections, but does not greatly change either the general energy dependence of the cross sections or the relative $^{16}O+^{40}Ca$ and $^{16}O+^{44}Ca$ cross sections. As an example of the sensitivity of the calculations to the diffuseness parameter, for the $^{16}O+^{40}Ca$ reaction at $E_{c.m.}=60.7$ MeV an increase of Δ from $2\hbar$ to $2.5\hbar$ results in the calculated fission cross section increasing from 71 mb to 95 mb, while maintaining a constant ER cross section. The present experiment was unable to follow the fission-like yield to the more asymmetric mass partitions, and considering the sensitivity of the magnitude of the calculated yield to the parameter Δ which, *a priori*, is not well known, it is not possible to directly compare the magnitude of the calculated cross sections to the experimental cross sections. It is interesting, however, that a substantial fission cross section is predicted. The calculated cross sections would probably be even greater if the fission barriers appropriate for the asymmetric mass partitions, which appear favored experimentally, were used in the calculation rather than the symmetric barriers actually employed. It is clear that the overall energy dependence of the cross sections for the two systems is well reproduced by the CASCADE calculations.

E. Deep-inelastic scattering calculations

In the preceding discussion it has been shown that the large-angle, strongly-damped yields from the $^{16}O+^{44}Ca$ reactions can be understood in terms of a fusion-fission model; as indicated, however, many of the features of the data may also result from a deep-inelastic scattering, orbiting process. To explore this latter possibility further, model calculations of the deep-inelastic process have been made using a computer code developed by Feldmeier.[36] In these calculations a semiclassical model[36,37] is used to determine the mean and variance of the mass drift, the final total kinetic energy, and the scattering angle as functions of the impact parameter for the interactions between two nuclei.

The calculations follow the evolution of the shapes of the interacting nuclei as they come together, form a connecting neck, and then either reseparate or fuse into a compound nucleus. Before the two nuclei touch, Randrups's proximity window formula[38] is used to obtain the dissipative force. During the time that a neck connects the two nuclei, one-body dissipation is introduced by a combination of the wall and window formulations.[39] By following these calculations as a function of the initial relative angular momentum (impact parameter), a Wilczynski-plot trajectory is obtained.

The Wilczynski trajectory for the $^{16}O+^{40}Ca$ reaction at $E_{c.m.}=60.7$ MeV is shown in Fig. 10. For angular momenta $l\leq 35\hbar$ the system is found to become trapped behind the fission barrier and fuses. At $l=36\hbar$, the first partial wave for which the system does not undergo fusion, the scattering is to a relatively forward, negative angle—there is no evidence for an orbiting component which might account for the observed angular distributions. Also, the calculated mass distributions for the

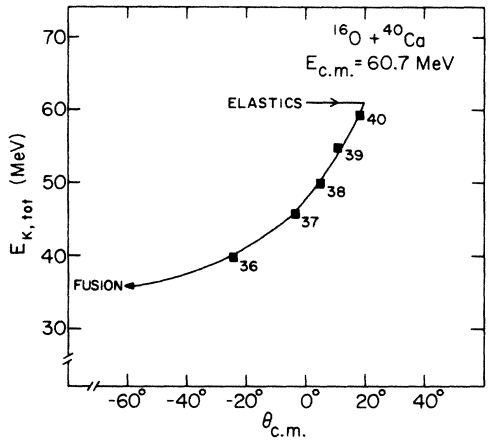

FIG. 10. Wilczynski-plot trajectory calculated for the $^{16}O+^{40}Ca$ reaction at $E_{c.m.}=60.7$ MeV using a deep-inelastic scattering model of the interaction. The positions on the trajectory for l values between 36 and 40, inclusive, are indicated.

$l=36\hbar$ partial wave, as indicated by the dashed line in Fig. 8, is found to be shifted only slightly from the incoming mass asymmetry and has a width which is narrower than that indicated by the experimental results. For $l>36\hbar$, the calculated mass distributions become even narrower, and the predicted final total kinetic energy is inconsistent with our measurements.

The failure of the model calculations to describe our experimental results may argue against a deep-inelastic scattering origin for the observed yields. It should be noted, however, that the model used in the present, parameter-free calculations was developed for heavier systems and assumes sharp nuclear surfaces. In an analysis of the $^{12}C+^{40}Ca$, $^{8}Be+^{40}Ca$, and $^{6}Li+^{40}Ca$ data of Grotowski *et al.*[10] within the framework of the coalescence and reseparation model, Błocki *et al.*[40] have reached similar conclusions concerning the importance of the fusion-fission mechanism in relation to deep-inelastic scattering—although again sharp nuclear surfaces are assumed in their model of the nuclear dynamics. Whether a more explicit treatment of diffuse-surface effects, which are clearly important in light systems, would result in sufficiently enhanced dissipation to bring the calculations more in line with the experimental results in an open question.

V. CONCLUSIONS

In studying the fission-like yield of the $^{16}O+^{40}Ca$ and $^{16}O+^{44}Ca$ reactions it is found that many of the characteristic features of this yield for the two systems can be understood in terms of a fusion-fission model. The observed symmetric-fragment total kinetic energies for both systems are well reproduced in a model where the liquid drop saddle-point shapes are simulated by two spheroids. The schematic calculations of the mass distributions expected from a fusion-fission process also indicate that the observed distributions are consistent with such a process. However, since both the final total kinetic energies and

mass distributions are believed to be determined after the fission barrier has been penetrated, they cannot be used as evidence of passing through the barrier. More direct evidence of barrier penetration comes from the energy dependence of the observed fission-like yields. These yields track closely with the expected energy dependence of the fission cross sections as calculated for the compound ^{56}Ni and ^{60}Ni systems assuming that compound-nucleus fission competes with light-particle evaporation. This last argument could be greatly strengthened by more complete measurements of the total fission-like yield in these, and other light systems.

Calculations of the mass distribution and Wilczynski trajectory for the deep-inelastic scattering process were found to be inconsistent with the experimental results. The model used in these calculations, however, may have limited applicability in light systems where diffuse-surface effects are expected to be large.

The presence of a fusion-fission reaction mechanism in light systems could have a number of consequences. At higher energies, where fission is more likely, the assumption that the total fusion cross section can be equated with the evaporation-residue cross sections might need to be reevaluated. The competing roles of fusion-fission and deep-inelastic scattering also require further study. The great sensitivity of the magnitude of the calculated fission cross sections in these light systems to the diffuseness of the fusion l distribution suggests that fission measurements may be useful in exploring the high-l dependence of fusion. Finally, the present data and analysis are not at variance with the supposition of Ref. 14 in which a fission mechanism was invoked to explain the resonances observed in excitation functions for these reactions.

ACKNOWLEDGMENTS

The authors would like to acknowledge D. Henderson for assistance in the experiment, B. B. Back for many useful discussions, K. E. Rehm for help in running the deep-inelastic scattering code of H. T. Feldmeier, and D. A. Bromley for comments on the manuscript. One of us (R.R.B.) would like to thank K. Grotowski for helpful conversations. This work was performed under the auspices of the U.S. Department of Energy, Contract Nos. W-31-109-ENG-38 and AC02-76ER03074, and was also supported in part by the Danish Natural Science Research Council.

*Present address: Lawrence Berkeley Laboratory, Berkeley, CA 94720.

†Present address: Physics Department, University of Pennsylvania, Philadelphia, PA 19104.

‡Present address: Argonne National Laboratory, Argonne, IL 60439.

[1]H. Oeschler, P. Wagner, J. P. Coffin, P. Engelstein, and B. Heusch, Phys. Lett. **87B**, 193 (1979).

[2]F. Plasil, T. C. Awes, B. Cheynis, D. Drain, R. L. Ferguson, F. E. Obershain, A. J. Sierk, S. G. Steadman, and G. R. Young, Phys. Rev. C **29**, 1145 (1984), and references therein.

[3]B. B. Back, R. R. Betts, J. E. Gindler, B. D. Wilkins, S. Saini, M. B. Tsang, C. K. Gelbke, W. G. Lynch, M. A. McMahan, and P. A. Baisden, Phys. Rev. C **32**, 195 (1985), and references therein.

[4]C. K. Gelbke, P. Braun-Munzinger, J. Barrette, B. Zeidman, M. J. Levine, A. Gamp, H. L. Harney, and Th. Walcher, Nucl. Phys. **A269**, 460 (1976).

[5]H. Doubre, A. Gamp, J. C. Jacmart, N. Poffe, J. C. Roynette, and J. Wilczynski, Phys. Lett. **73B**, 135 (1978).

[6]P. Wastyn, H. Feldmeier, F. Beck, M. Dworzecka, H. Genz, M. Mutterer, A. Richter, G. Schrieder, and J. P. Theobald, Nucl. Phys. **A332**, 455 (1979).

[7]J. Carter, H. Feldmeier, A. Richter, G. Schrieder, and P. Wastyn, Z. Phys. A **302**, 365 (1981).

[8]J. Carter, C. Brendel, A. Richter, G. Schrieder, H. Feldmeier, W. Bohne, K. Grabisch, H. Lehr, and H. Morgenstern, Z. Phys. A **313**, 57 (1983).

[9]H. Lehr, W. Bohne, K. Grabisch, H. Morgenstern, and W. Von Oertzen, Nucl. Phys. **A415**, 149 (1984).

[10]K. Grotowski, Z. Majka, R. Płaneta, M. Szczodrak, Y. Chan, G. Guarino, L. G. Moretto, D. J. Morrissey, L. G. Sobotka, R. G. Stokstad, I. Tserruya, S. Wald, and G. J. Wozniak, Phys. Rev. C **30**, 1214 (1984).

[11]R. R. Betts, in *Proceedings of the Conference on Resonances in Heavy Ion Reactions, Bad Honnef, West Germany, 1981,* Vol. 156 of *Lecture Notes in Physics,* edited by K. A. Eberhardt (Springer, Berlin, 1981), p. 185.

[12]R. Ritzka, W. Dünnweber, A. Glaesner, W. Hering, H. Puchta, and W. Trautmann, Phys. Rev. C **31**, 133 (1985).

[13]T. C. Awes, R. L. Ferguson, R. Novotny, F. E. Obenshain, F. Plasil, V. Rauch, G. R. Young, and H. Sann, Phys. Rev. Lett. **55**, 1062 (1985).

[14]R. R. Betts, in *Proceedings of the 5th Adriatic International Conference on Nuclear Physics, Hvar, Yugoslavia, 1984,* edited by N. Cindro, W. Greiner, and R. Caplar (World Scientific, Singapore, 1984), p. 33.

[15]T. Bengtsson, M. Faber, M. Ploszajczak, I. Ragnarsson, and S. Åberg, Lund Institute of Technology Report No. MPh-84/01, and private communication.

[16]F. Plasil and R. L. Ferguson, in *Proceedings of the International Symposium on Physics and Chemistry of Fission, Jülich, 1979* (IAEA, Vienna, 1980), p. 521, and references therein.

[17]S. B. Kaufman, E. P. Steinberg, B. D. Wilkins, J. Unik, and A. J. Gorski, Nucl. Instrum. Methods **115**, 47 (1974).

[18]S. E. Vigdor, D. G. Kovar, P. Sperr, J. Mahoney, A. Menchaca-Rocha, C. Olmer, and M. S. Zisman, Phys. Rev. C **20**, 2147 (1979).

[19]B. K. Dichter, Ph.D. thesis, Yale University, 1985 (unpublished).

[20]I. Halpern, V. M. Strutinski, in *Proceedings of the Second United Nations International Conference on the Peaceful Uses of Atomic Energy* (United Nations, Geneva, 1958), p. 408.

[21]D. Shapira, R. Novotny, Y. D. Chan, K. A. Erb, J. L. C. Ford, Jr., J. C. Peng, and J. D. Moses, Phys. Lett. **114B**, 111 (1982).

[22]R. Vandenbosch and J. R. Huizenga, *Nuclear Fission* (Academic, New York, 1973).

[23]R. R. Betts and S. B. DiCenzo, Phys. Rev. C **19**, 2070 (1979).
[24]K. T. R. Davies, R. A. Managan, J. R. Nix, and A. J. Sierk, Phys. Rev. C **16**, 1890 (1977).
[25]J. R. Nix, Nucl. Phys. **A130**, 241 (1969).
[26]K. T. R. Davies and J. R. Nix, Phys. Rev. C **14**, 1977 (1976).
[27]A. J. Sierk, Phys. Rev. C **33**, 2039 (1986).
[28]K. T. R. Davies and J. R. Nix, Phys. Rev. C **14**, 1977 (1976).
[29]H. J. Krappe, J. R. Nix, and A. J. Sierk, Phys. Rev. C **20**, 992 (1979).
[30]M. G. Mustafa, P. A. Baisden, and H. Chandra, Phys. Rev. C **25**, 2524 (1982).
[31]L. G. Sobotka, M. A. McMahan, R. J. McDonald, C. Signarbieux, G. J. Wozniak, M. L. Padgett, J. H. Gu, Z. H. Liu, Z. Q. Yao, and L. G. Moretto, Phys. Rev. Lett. **53**, 2004 (1984).
[32]D. R. Saroha, N. Malhotra, and R. K. Gupta, J. Phys. G **11**, L27 (1985).
[33]B. D. Wilkins, E. P. Steinberg, and R. R. Chasman, Phys. Rev. C **14**, 1832 (1976).
[34]W. D. Myers and W. J. Swiatecki, Ann. Phys. (N.Y.) **84**, 186 (1974); parameters given by W. D. Myers, *Droplet Model of Atomic Nuclei* (Plenum, New York, 1977).
[35]F. Pühlhofer, Nucl. Phys. **A280**, 267 (1977), and private communication concerning modification of the computer code CASCADE for corrections in the fission competition option.
[36]H. T. Feldmeier, Argonne National Laboratory Report No. ANL-PHY-85-2, 1985 (unpublished).
[37]J. Błocki, M. Dworzecka, F. Beck, and H. Feldmeier, Phys. Lett. **99B**, 13 (1981).
[38]F. Beck, J. Błocki, M. Dworzecka, and G. Wolschin, Phys. Lett. **76B**, 35 (1978).
[39]J. Błocki, Y. Boneh, J. R. Nix, J. Randrup, M. Robel, A. J. Sierk, and W. J. Swiatecki, Ann. Phys. (N.Y.) **113**, 330 (1978).
[40]J. Błocki, K. Grotowski, R. Płaneta, and W. J. Swiatecki, Nucl. Phys. **A445**, 367 (1985).